This document is the accepted manuscript version of the following article:
Tomonaga, Y., Yagasaki, K., Park, J. O., Ashi, J., Toyoda, S., Takahata, N., & Sano, Y. (2020). Fluid dynamics along the Nankai Trough: he isotopes reveal direct seafloor mantle-fluid emission in the Kumano Basin (Southwest Japan). ACS Earth and Space Chemistry, 4(11), 2105-2112.https://doi.org/10.1021/acsearthspacechem.0c00229

Fluid dynamics along the Nankai Trough: He isotopes reveal direct seafloor mantle-fluid emission in the Kumano Basin (southwest Japan)

Yama Tomonaga,*,†,‡ Kazuhiro Yagasaki,† Jin-Oh Park,† Juichiro Ashi,† Shin Toyoda,¶ Naoto Takahata,† and Yuji Sano†,§

†*Atmosphere and Ocean Research Institute, The University of Tokyo, 5-1-5 Kashiwanoha, Kashiwa-shi, Chiba 277-8564, Japan*

‡*Eawag, Swiss Federal Institute of Aquatic Science and Technology, Department of Water Resources and Drinking Water, Ueberlandstrasse 133, CH-8600 Duebendorf, Switzerland*

¶*Department of Applied Physics, Okayama University of Science, Okayama, Japan*

§*Institute of Surface-Earth System Science, Tianjin University, Tianjin 300072, P.R. China*

E-mail: yama@tomonaga.ch

Abstract

We collected bottom water samples and unconsolidated sediment samples for noble-gas analysis in the water column as well as in the pore water phase along the Nankai Trough to assess the sources and the fluxes of seafloor fluid emission at the local/regional scale.

The results indicate that the terrigenic He emission is rather variable in terms

of fluxes and isotope signatures. The largest He fluxes are detected at a previously investigated cold seep site where terrigenic He is mainly of crustal origin.

High He isotope ratios detected at shallower depths in the Kumano Basin indicate that mantle fluids are able to migrate from the deep sediment column up to the seafloor. Our findings are in line with the detection of mantle He in fluids recovered by IODP deep-drilling operations and make the case that even seafloor volatile screening and monitoring might provide useful insights on the relation between fluid dynamics and tectonic/seismic activity in the investigated region for future forecasting of earthquakes.

Keywords: volatile emission, noble gases, mantle fluids, unconsolidated sediments, Nankai Trough

Introduction

Noble-gas geochemistry (in particular the He isotope signature) is known to change in response to the terrigenic fluid emission (i.e., emission of fluids originating from the solid earth) triggered by major seismic events, as observed, for instance, in the recent case of the Tohoku-Oki earthquake in 2011[1] or the Kumamoto earthquake in 2016.[2] However, the interpretation of volatile anomalies in relation to seismic events depends strongly on the investigated geological setting and the available geochemical information.[3] Therefore, characterizing the terrigenic fluid emission in tectonically active regions by empirical observations on a regular basis is a prerequisite to understand future geochemical changes produced in relation to seismicity.[4,5] This may sound trivial for continental regions, but the collection of data at the ocean floor remains a challenging task in terms of financial and technical resources. Indeed, only a very limited number of studies provide noble-gas measurements in the pore water of ocean sediments.[6–12]

Here we report the results of the noble-gas analyses conducted in water and sediment samples collected by ROV along the Nankai Trough (Fig. 1). From the measured He isotope

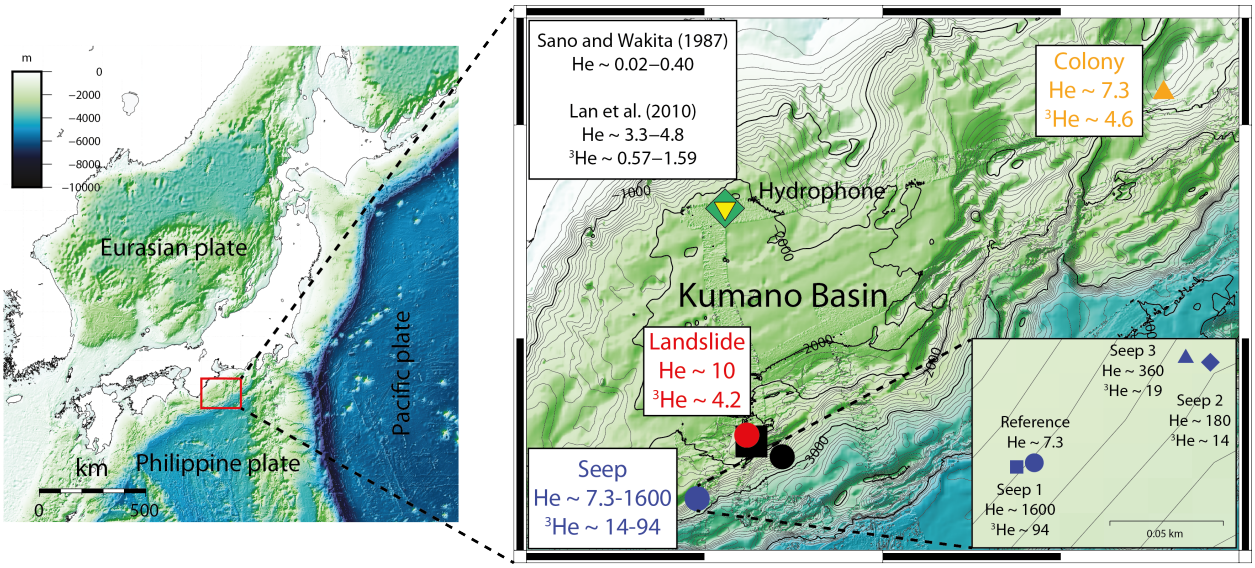

Figure 1: Sampling locations during RV Natsushima cruises NT13-08 and NT14-07. The same symbols are used in Figs. 2 and 3 to distinguish the measurements at each site. At the Hydrophone (green rhomboid, yellow triangle) and S-E Landslide (black square, black circle) stations only water samples have been collected. The total He fluxes (in 10^9 atoms/m^2/s) and the ^{3}He fluxes (in 10^4 atoms/m^2/s) at each location are estimated, whenever possible, from the concentration gradients determined in the sediment pore water (Fig. 2). In the Seep region strong He flux variations are observed within a few tens of meters. Similar total He fluxes may imply similar fluid transport mechanisms (i.e., diffusion vs. advection).

concentrations we provide first estimates of the He fluxes at the sampling locations in the non-volcanic forearc region. Noble-gas concentrations and isotope signatures are discussed considering the respective geodynamic context.

Methods

Study site

The Nankai Trough is located in the southwest of Japan where the Philippine Sea Plate subducts beneath the Eurasian Plate at a rate of about 4–7 cm/yr.[13,14] The region is known for its active seismicity and during the last decades hydrologic observatories were installed in deep-driling boreholes to monitor e.g. changes in pore-fluid pressure resulting from tectonic movements.[15]

Hence, the emission of terrigenic fluids is expected in this region. However, studies of noble gases in pore fluids and their migration in the sediment column are rather scarce even considering the whole island arc of Japan. Sano and Wakita determined He isotope abundances in the pore water of deep-drilling sediments at two sites in the Nankai Trough and at the Japan Trench.[9] In the Nankai Trough the $^3He/^4He$ ratios ranged from 0.3 Ra (i.e., the measured $^3He/^4He$ ratio of $0.4 \cdot 10^{-6}$ normalized by the $^3He/^4He$ ratio of atmospheric air, Ra,[16] of $1.39 \cdot 10^{-6}$) up to 0.9 Ra ($^3He/^4He = 1.2 \cdot 10^{-6}$) while at the Japan Trench they were found to be 0.2-0.8 Ra ($^3He/^4He = (0.3 - 1.1) \cdot 10^{-6}$). The ^4He fluxes estimated for the Nankai Trough and the Japan Trench were $0.02 \cdot 10^9$ atoms/m^2/s and $0.4 \cdot 10^9$ atoms/m^2/s, respectively. Lan et al. determined ^4He and ^3He fluxes at the Mid-Okinawa Trough back-arc basin to be $(3.3 - 4.8) \cdot 10^9$ atoms/m^2/s and $(0.6 - 1.6) \cdot 10^4$ atoms/m^2/s, respectively.[8] The $^3He/^4He$ ratios measured by Lan et al. ranged from 1.1 Ra up to 2.0 Ra. Other studies targeting the geochemical characterization of pore fluids by He isotope composition and the quantification of He fluxes are, at least to our knowledge, not available.

Toki et al. reported high crustal-derived He shares (resulting in $^3He/^4He$ ratios of ap-

proximately 0.1 Ra) measured in pore water samples collected at cold seeps at Oomine Ridge in the Nankai Trough.[11] More recently, Wiersberg et al. reported mantle-derived helium in the deep sediment column of the Kumano forearc basin.[17] The $^3He/^4He$ ratios, measured in deep-drilling mud gas samples, were up to 3.3 Ra. In the same work the authors presented Ne and Ar isotope ratios being, however, not distinguishable from the respective atmospheric values. The gas chemistry was also found to be very similar to air with a slight methane excess. Wiersberg et al. discussed the presence of mantle He in terms of diffusive fluid transport trough the accretionary prism. However, no terrigenic He fluxes could be inferred.

In this work, three regions where sediment samples could be collected are labeled as Seep, Landslide, and Colony (see Fig. 1). The Seep site corresponds to the area characterized by the cold seepage mentioned in Toki et al..[11,18] The Landslide site is located in the proximity of IODP Site C0002 investigated by Wiersberg et al..[17] The Colony site, located in the outer ridge off Tokai, is characterized by the presence of a large-scale Calyptogena colony along the Daini Tenryu knoll being comprised mainly of dead shells with very few "patches" of living bivalves remaining.[19,20] The observation of such a bivalve colony is indicative of an active seepage providing nutrient-rich fluids (e.g., methane and various sulphides) on which these chemosynthetic organisms can feed.

Noble-gas sampling and analysis

Ocean bottom water and sediment cores were collected during RV Natsushima cruises NT13-08 and NT14-07 (managed by JAMSTEC) using the ROV Hyper-Dolphin equipped with Nisking bottles and an MBARI corer.

Immediately after termination of each dive, water was transferred without exposure to the atmosphere from the Niskin bottles into 60-cm-long copper tubes. Both ends of the copper tubes were sealed airtight by two steel clamps for storage.[21]

Sediment samples were acquired using the technique of Brennwald et al.[22] to sample noble gases in unconsolidated sediment. Immediately after core recovery, the bulk sediment was

transferred into small copper tubes by squeezing the sediment core with two pistons moving along the axis of the plastic liner. The copper tubes, attached to the side of the liner using Swagelok fittings (i.e., at different coring depths), were filled with bulk sediment. After being flushed with a certain amount of sediment, the copper tubes were sealed airtight by closing two metal clamps.[22–25] Sample preparation in the laboratory was carried out according to the method of Tomonaga et al..[12,24,26] Each original sample was divided into two aliquots by placing two pairs of additional metal clamps (each pair being kept at the same distance of 9.5 cm using a metal holder). Each aliquot was then centrifuged to separate the pore water from the sediment matrix. Centrifugation was conducted using a fixed-angle rotor for 4 h at 7500 rpm. To avoid deformation of the copper tubes during centrifugation, they are held in place by custom-made polypropylene supports. Prior to each centrifuging step, the samples were put in an ultrasonic bath for 30 minutes to loosen the bulk sediment matrix from the copper tube wall. After centrifugation, the first aliquot was opened to determine the position of the sediment-water interface. The second aliquot was split at the position of the sediment-water interface with a third clamp. Thereafter, the pore water and the compressed sediment phase were completely separated from each other.

Noble-gas analysis was conducted on the bulk water (ocean bottom water samples) or the separated pore water (sediment samples) according to the well-established experimental protocols commonly used to determine noble-gas abundances in water samples.[21] In the laboratory, the samples were connected to a high-vacuum line with a lead glass container to extract the dissolved gases from the pore water based on the displacement method. The exsolved gases were transferred from the glass bottle into a purification line where He was purified using hot titanium-zirconium getters and charcoal traps held at liquid nitrogen temperature. The $^{20}Ne/^{4}He$ ratios were measured by an online quadrupole mass spectrometer (QMS 100 by Pfeiffer). Subsequently, He was separated from Ne (and other residual gas species) using a cryogenic charcoal trap held at 40 K.[27] The $^{3}He/^{4}He$ ratios were determined using a noble gas mass spectrometer (Helix-SFT by GV Instruments) and calibrated

against the He Standard of Japan (HESJ[28]) at the Atmosphere and Ocean Research Institute (AORI), The University of Tokyo. Blank measurements were performed prior to the sample measurements. The intensities of the blanks were about three orders of magnitude lower than the typical sample intensities. Therefore, a blank correction was not applied. The reproducibility of the standard measurements was better than 2% for the QMS 100 and better than 1% for the Helix-SFT. For the concentration measurements, the average experimental errors were 4% (^{3}He), 6% (^{4}He), and 3% (^{20}Ne). The average experimental errors of the isotope ratios were 3% (^{3}He/^{4}He) and 6% (^{20}Ne/^{4}He).

Estimation of the He fluxes

A first-order estimation of the diffusive He fluxes (F) was performed according to Fick's law: $F = -D \cdot \partial C/\partial z$ where D is the molecular diffusion coefficient of He in bulk water for the in-situ temperature and salinity conditions and $\partial C/\partial z$ is the He concentration gradient determined by linear regression of the measured He concentration profile at each sampling position.

The determination of terrigenic He fluxes provides quantitative information on the intensity of the local/regional terrigenic fluid emission. Such information can be used to infer the relevant transport mechanisms (i.e., diffusion vs. advection) and, in combination with the geochemical characterization of the emitted fluids, to assess future relations to seismicity in tectonically active regions.

Results and discussion

The results of the noble-gas measurements conducted in water and sediment samples collected along the Nankai Trough are summarized in Table 1.

As the investigated sediment depths are very shallow, the slowest transport process is likely to be close to molecular diffusion in bulk water. The top boundary condition for the

Table 1: Sampling location details and results of the noble-gas measurements conducted in water (H2O) and sediment (SED) samples collected along the Nankai Trough. STP = standard temperature (0°C) and pressure (1 atm).

Cruise	Date	Dive #	Location	Position [°N]	Position [°E]	Water depth [m]	Sediment depth [m]	Temp. [°C]	Salinity [PSU]	Sample type	^{3}He [10^{-14} cm^3_{STP}/g]	^{4}He [10^{-8} cm^3_{STP}/g]	^{20}Ne [10^{-7} cm^3_{STP}/g]	^{3}He/^{4}He [10^{-6}]	^{20}Ne/^{4}He [-]
NT13-08	04/14/13	1513	Landslide	33.2209	136.7179	2596		1.6	34.6	H2O	7.31 ± 0.05	4.26 ± 0.03	1.636 ± 0.004	1.71 ± 0.01	3.84 ± 0.03
	04/15/13	1514	Seep	33.1223	136.4792	2552		1.7	34.6	H2O	7.11 ± 0.07	4.30 ± 0.04	1.648 ± 0.004	1.65 ± 0.02	3.83 ± 0.04
	04/15/13	1514	Seep	33.1223	136.4792	2552		1.7	0.0	H2O	7.0 ± 0.5	4.0 ± 0.5	1.57 ± 0.06	1.7 ± 0.2	3.9 ± 0.5
	04/15/13	1514	Seep	33.1223	136.4792	2552	0.05	1.7	34.6	SED	9.4 ± 0.3	7.9 ± 0.3	1.63 ± 0.03	1.19 ± 0.04	2.08 ± 0.09
	04/15/13	1514	Seep	33.1223	136.4792	2552	0.11	1.7	34.6	SED	4.2 ± 0.2	4.3 ± 0.3	0.60 ± 0.03	0.97 ± 0.05	1.4 ± 0.1
	04/15/13	1514	Seep	33.1223	136.4791	2549		1.6	34.6	H2O	7.29 ± 0.06	4.20 ± 0.04	1.617 ± 0.004	1.73 ± 0.01	3.85 ± 0.04
	04/15/13	1514	Seep	33.1223	136.4791	2549		1.6	34.6	H2O	7.5 ± 0.5	4.5 ± 0.4	1.80 ± 0.05	1.65 ± 0.01	4.0 ± 0.4
	04/15/13	1514	Seep	33.1223	136.4791	2549	0.11	1.6	34.6	SED	73.1 ± 0.8	131 ± 1	1.57 ± 0.02	0.56 ± 0.01	0.120 ± 0.002
	04/15/13	1514	Seep	33.1223	136.4791	2549	0.03	1.6	34.6	SED	31.4 ± 0.6	55 ± 1	1.62 ± 0.03	0.57 ± 0.01	0.29 ± 0.01
	04/16/13	1515	Landslide	33.2571	136.6316	2123		1.7	34.6	H2O	7.26 ± 0.07	4.21 ± 0.05	1.615 ± 0.005	1.72 ± 0.02	3.84 ± 0.04
	04/16/13	1515	Landslide	33.2571	136.6316	2123		1.7	34.6	H2O	6.3 ± 0.5	3.7 ± 0.4	1.57 ± 0.06	1.7 ± 0.2	4.2 ± 0.5
	04/16/13	1515	Landslide	33.2722	136.6183	1975		1.7	34.6	H2O	6.79 ± 0.07	3.97 ± 0.04	1.526 ± 0.003	1.71 ± 0.02	3.84 ± 0.04
	04/16/13	1515	Landslide	33.2722	136.6183	1975		1.7	34.6	H2O	7.1 ± 0.4	4.3 ± 0.4	1.75 ± 0.05	1.66 ± 0.01	4.1 ± 0.4
	04/16/13	1515	Landslide	33.2722	136.6183	1980	0.04	1.7	34.6	SED	11.5 ± 0.4	5.7 ± 0.2	1.71 ± 0.03	2.00 ± 0.07	3.0 ± 0.1
	04/16/13	1515	Landslide	33.2722	136.6183	1980	0.10	1.7	34.6	SED	13.2 ± 0.4	6.1 ± 0.2	1.62 ± 0.03	2.15 ± 0.07	2.6 ± 0.1
	04/16/13	1515	Landslide	33.2722	136.6183	1980	0.16	1.7	34.6	SED	8.4 ± 0.3	4.9 ± 0.2	1.66 ± 0.02	1.71 ± 0.06	3.4 ± 0.1
	04/16/13	1515	Landslide	33.2722	136.6183	1980	0.22	1.7	34.6	SED	15.4 ± 0.5	6.5 ± 0.2	1.57 ± 0.03	2.4 ± 0.1	2.4 ± 0.1
NT14-07	04/23/14	1653	Hydrophone	33.8049	136.5577	2039		2.0	34.6	H2O	7.2 ± 0.4	4.3 ± 0.4	1.65 ± 0.05	1.68 ± 0.01	3.8 ± 0.4
	04/24/14	1654	Seep	33.1227	136.4800	2560		1.6	34.6	H2O	7.8 ± 0.5	4.7 ± 0.4	1.89 ± 0.06	1.67 ± 0.01	4.0 ± 0.4
	04/24/14	1654	Seep	33.1227	136.4800	2560	0.16	1.6	34.6	SED	22.3 ± 0.5	26.8 ± 0.7	1.55 ± 0.04	0.83 ± 0.02	0.58 ± 0.02
	04/25/14	1655	Colony	34.0757	137.7884	610		5.6	34.3	H2O	6.6 ± 0.4	4.3 ± 0.4	1.69 ± 0.05	1.54 ± 0.01	4.0 ± 0.4
	04/25/14	1655	Colony	34.0757	137.7884	610		5.6	34.3	H2O	7.2 ± 0.4	4.5 ± 0.4	1.84 ± 0.05	1.58 ± 0.01	4.1 ± 0.4
	04/25/14	1655	Colony	34.0757	137.7885	611	0.07	5.3	34.3	SED	8.9 ± 0.4	4.8 ± 0.2	1.70 ± 0.05	1.85 ± 0.08	3.5 ± 0.2
	04/25/14	1655	Colony	34.0757	137.7885	611	0.13	5.3	34.3	SED	17 ± 1	5.6 ± 0.7	1.5 ± 0.2	3.0 ± 0.4	2.7 ± 0.5
	04/25/14	1655	Colony	34.0757	137.7885	611	0.19	5.3	34.3	SED	9.4 ± 0.6	5.1 ± 0.4	1.52 ± 0.07	1.8 ± 0.2	3.0 ± 0.2
	04/26/14	1656	Hydrophone	33.8050	136.5574	2040		2.0	34.6	H2O	7.2 ± 0.4	4.4 ± 0.4	1.73 ± 0.05	1.63 ± 0.01	3.9 ± 0.4
	04/27/14	1657	Seep	33.1227	136.4799	2558		1.7	34.6	H2O	7.2 ± 0.4	4.4 ± 0.4	1.74 ± 0.05	1.63 ± 0.01	3.9 ± 0.4
	04/27/14	1657	Seep	33.1227	136.4799	2558	0.02	1.7	34.6	SED	9.1 ± 0.6	8.5 ± 0.7	1.90 ± 0.06	1.07 ± 0.01	2.2 ± 0.2

fluid transport in the pore space is given by the bottom seawater, where conditions close to air-saturated water (ASW) prevail (i.e., no or rather low terrigenic He excesses). As molecular diffusion of He in bulk water is relatively fast, diffusion-controlled transport is expected to result in (very) low He concentration gradients in the pore water close to the sediment/water interface. Therefore, the observation of high He concentration gradients is indicative of an advective transport component.

The sediment cores acquired at the active cold seep site at the splay fault[29] off-shore Kumano (labeled as Seep in Fig. 1, blue symbols) previously investigated by Toki et al.[11] are characterized by a broad range of He concentration gradients (Fig.2). The highest He fluxes in this cold seep region (up to $1600 \cdot 10^9$ atoms/m^2/s for ^{4}He and $94 \cdot 10^4$ atoms/m^2/s for ^{3}He) indicate the presence of advection affecting the overall fluid transport.

Sediment cores collected at shallower water depths in the Kumano Basin and in the outer ridge off Tokai (labeled as Landslide and Colony in Fig. 1, red and orange symbols) show rather low He concentration gradients. The respective He fluxes are low and similar ($(7.3 - 10) \cdot 10^9$ atoms/m^2/s for ^{4}He and $(4.2 - 4.6) \cdot 10^4$ atoms/m^2/s for ^{3}He) suggesting a diffusion-controlled He emission. It should be noted, however, that even these low He fluxes are higher than the ones determined by previous works[8,9] in the same forearc region. From this observation it cannot be excluded that minor advective component is present also at these sites. Based on the relatively low He flux at the Colony site we speculate that a large Calyptogena community observed at the same location[19,20] flourished under more active seepage conditions prevailing in the past.

The measured ^{3}He/^{4}He ratios (Fig. 3) are highly variable in space and highlight the complexity of the emission of terrigenic fluids within the studied region. The Seep site is characterized by low ^{3}He/^{4}He ratios (Fig. 3, blue symbols). Such low ^{3}He/^{4}He ratios underline the prevalence of crustal He and are in line with the findings of Toki et al..[11] In contrast, the high ^{3}He/^{4}He ratios determined in cores collected at shallower water depths (Fig. 3, red and orange symbols) indicate the admixture of a significant share of mantle He.

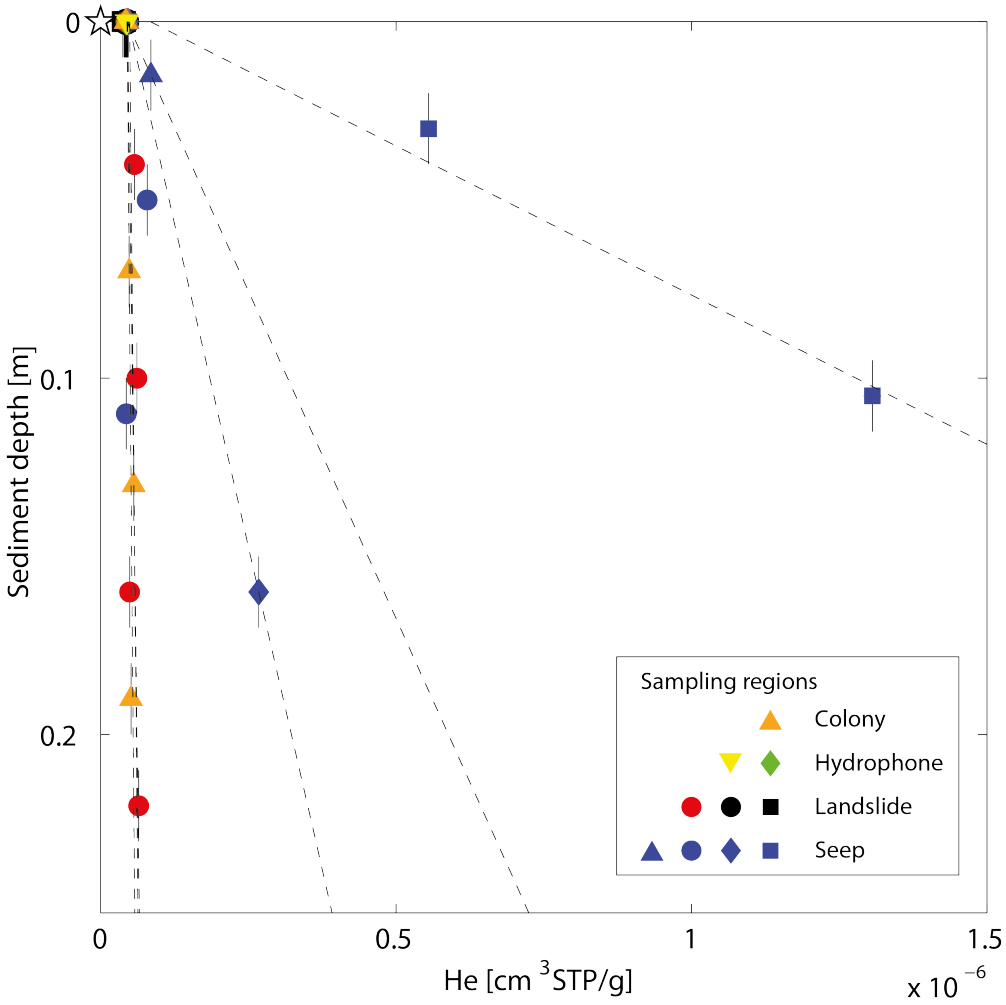

Figure 2: Cold seep sites (blue symbols) are characterized by highly variable He concentrations gradients. At the Landslide and Colony stations (red and orange symbols), located at shallower water depths, low He concentration gradients are observed. The open star indicates the He concentrations for air-saturated water (ASW) calculated for the local salinity and temperature conditions.

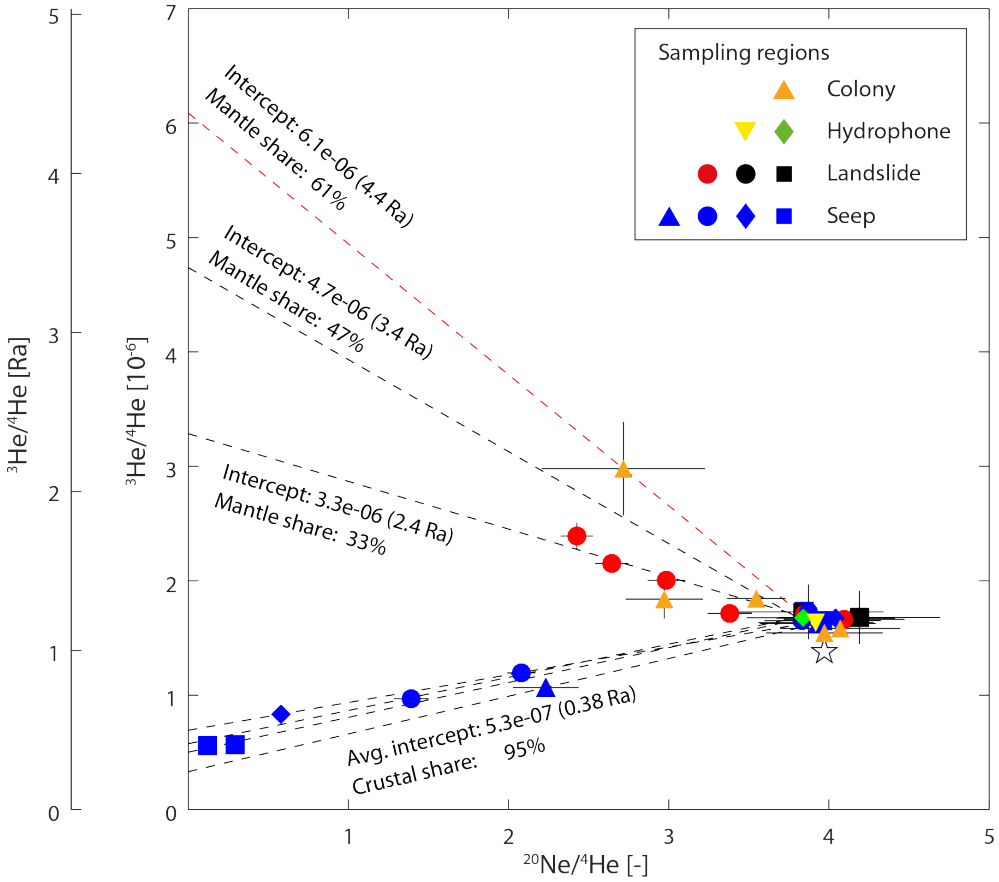

Figure 3: The three-isotope diagram depicts the distinct fluid origin at the respective locations. For $^{20}Ne/^{4}He = 0$ the intercept of the linear regressions (dashed lines) on the ordinate indicates the $^{3}He/^{4}He$ ratio of the source of terrigenic He for each site. The proportions of terrigenic He in the figure are calculated assuming a binary mixture of mantle and crustal He. The open star indicates the He isotope ratio for air-saturated water (ASW).

The origin of the fluids emitted at each site can be investigated more in detail using a so-called "three isotopes plot"[30] showing the relationship between the measured $^{20}Ne/^{4}He$ ratios and the $^{3}He/^{4}He$ ratios (Fig. 3). A majority of the determined $^{20}Ne/^{4}He$ ratios is ASW-like indicating the presence of a large share of atmospheric noble gases in the fluids. As the production of ^{20}Ne in the solid earth can be considered as negligible, the intercept on the ordinate axis (i.e., for $^{20}Ne/^{4}He = 0$) of the linear regressions based on the data set of each core indicate the $^{3}He/^{4}He$ composition of the source (R_s) of the emitted fluids at each location (i.e., without the contribution of atmospheric He). The proportions of mantle (p_m) and crustal (p_c) He can be inferred from the binary relation $R_s = p_m \cdot R_m + p_c \cdot R_c$ with $p_m + p_c = 1$. R_m and R_c are the typical $^{3}He/^{4}He$ ratios for mantle and crustal He of 10^{-5} and 10^{-8}, respectively.

The linear regressions marked by dashed black lines in Fig. 3 are based on the He isotope ratios measured in all samples of each core. The highest $^{3}He/^{4}He$ isotope ratio inferred from these regressions is 3.4 Ra ($^{3}He/^{4}He = 4.7 \cdot 10^{-6}$). It should be noted, however, that a regression line fitting the points with the lowest and the highest measured $^{3}He/^{4}He$ ratios at the Colony site (Fig. 3, red dashed line) would result in a $^{3}He/^{4}He$ ratio at the source of the emitted terrigenic fluids of about 4.4 Ra ($^{3}He/^{4}He = 6.1 \cdot 10^{-6}$). Such He isotope ratio is unusually high for a non-volcanic area and is the highest ratio ever reported in the investigated forearc region. Previously, $^{3}He/^{4}He$ ratios of up to 3.6 Ra have been measured in hot springs of Shikoku Island.[31,32] Such observation agrees well with the 3.3 Ra reported recently by Wiersberg et al.[17] but is significantly lower than the 4.4 Ra inferred from the data presented in this work.

The contribution of mantle He of up to approx. 60% (see Fig. 3) is larger than the one determined for the forearc region off-shore New Zealand of 20-30% with a $^{3}He/^{4}He$ ratio at the fluid origin of up to 2.5 Ra.[12] For the continental forearc region of New Zealand, the highest $^{3}He/^{4}He$ ratio reported is 3 Ra.[32,33] Thus, the 4.4 Ra determined in the present work remains the highest He isotope ratio ever determined in a forearc environment.

It should be noted that, in principle, the ^{3}He enrichment (approximately $1.1{\cdot}10^{-13}\,\mathrm{cm^3_{STP}/g}$ in excess with respect to the expected ASW value of $5.3 \cdot 10^{-14}\,\mathrm{cm^3_{STP}/g}$) in the sample with the highest ^{3}He/^{4}He ratio from the Colony site (^{3}He/^{4}He $= 3.0 \cdot 10^{-6}$) may be attributed to four different origins: 1) tritiogenic helium, 2) nucleogenic helium, 3) meteoritic helium, and 4) mantle helium.

Tritiogenic He can be ruled out, as tritium concentrations in deep seawater are very low and not sufficient to produce the observed ^{3}He excess. Indeed, the production of a similar ^{3}He excess would require the decay of about 46 TU (TU: tritium units; $1\,\mathrm{cm^3_{STP}/g}$ equals $4 \cdot 10^{14}$ TU[34]) or 5.4 Bq/L. Such ^{3}H concentration is at least one order of magnitude higher than the tritium concentrations possibly present in the ocean water at similar depths after the nuclear bomb peak in the 1960s[35] and higher than the ^{3}H concentrations measured in the ocean surface water after the Fukushima Dai-ichi nuclear accident in 2011 of up to 0.3 Bq/L.[36]

The presence of nucleogenic He is not likely, as nuclear reactions in the sediments should also produce large amounts of ^{4}He and the resulting ^{3}He/^{4}He ratios would be very low. The ^{3}He/^{4}He ratios measured at the Landslide and Colony sites clearly reject such an option.

The contribution of meteoritic He has been verified by measurements of the sediment matrix phase. The presence of large amounts of cosmic dust in the sediments is expected to result in high ^{3}He/^{4}He ratios. However, the ^{3}He/^{4}He ratios determined in the sediment matrix phase at the Landslide and Colony sites range from 0.15 Ra to 0.24 Ra indicating that meteoritic He is negligible.

The last possible source of ^{3}He is a mantle-derived component. According to the arguments listed above, the presence of mantle He is the only plausible explanation for the observed ^{3}He enrichment.

In previous studies, in order to explain 2-3 Ra in forearc regions of subduction zones, a slab component with an age-dependent radiogenic He ingrowth was considered.[32] Wiersberg et al.[17] agreed with the idea of slab aging and attributed the ^{3}He/^{4}He ratio of 3.3 Ra deter-

mined in the Kumano Basin to a remnant of mantle He in the young Philippine Sea Plate. The high $^3He/^4He$ ratios of 2–3 Ra in the forearc region of New Zealand were also explained by slab aging.[32] However, it is difficult to explain the $^3He/^4He$ ratio of 4.4 Ra inferred in the present work based on the concept of slab aging only.

The detection of mantle He emission at very shallow sediment depths (i.e., less than 30 cm) suggests the presence of preferential pathways for the release of deep-seated fluids. We propose two scenarios to explain the existence of such preferential pathways based on the 3D seismic reflection profiles available for the Landslide site (i.e., IODP Site C0002; Fig. 4). On the one hand, the megasplay fault may extend along the plate boundary fault fostering the horizontal migration of fluids from the mantle wedge to shallower depths (i.e., the Kumano Basin), eventually reaching the Landslide site (Fig. 4A). In a second scenario strike-slip faults may develop down into the subducting Philippine Sea Plate allowing the ascent of mantle fluids through vertically oriented preferential pathways (Fig. 4B). Indeed, the Landslide site belongs to the notch region (i.e., a trench-parallel depression along the seaward edge of the Kumano forearc basin and the upper slope of the accretionary prism) in which strike-slip faults could develop down to the upper mantle. Ashi et al.[38] discussed the development of strike-slip faults branched from a megathrust fault in the investigated area (but did not hypothesize their extension towards the mantle). A 3.5-km-wide weak reflectivity zone below the Landslide site is probably associated with intense fracturing because of persistent brittle strike-slip faulting. The fractured faults can provide the mentioned preferential pathways (please note the amplitude reduction of the plate boundary fault reflection within the weak reflectivity zone in Fig. 4B). Mantle-derived helium released through strike-slip faults has been reported in the San Andreas fault system[39,40] and the Yangsan fault in the Southeastern Korean Peninsula.[41] Helium and carbon isotopic changes determined across the Costa Rica convergent margin indicate pervasive deep slab and/or mantle degassing (i.e., also in the forearc region) that has been attributed to the presence of deep-penetrating faults.[42] Sano et al.[43] suggested the presence of a slab tear in the Kinki region and attributed very high

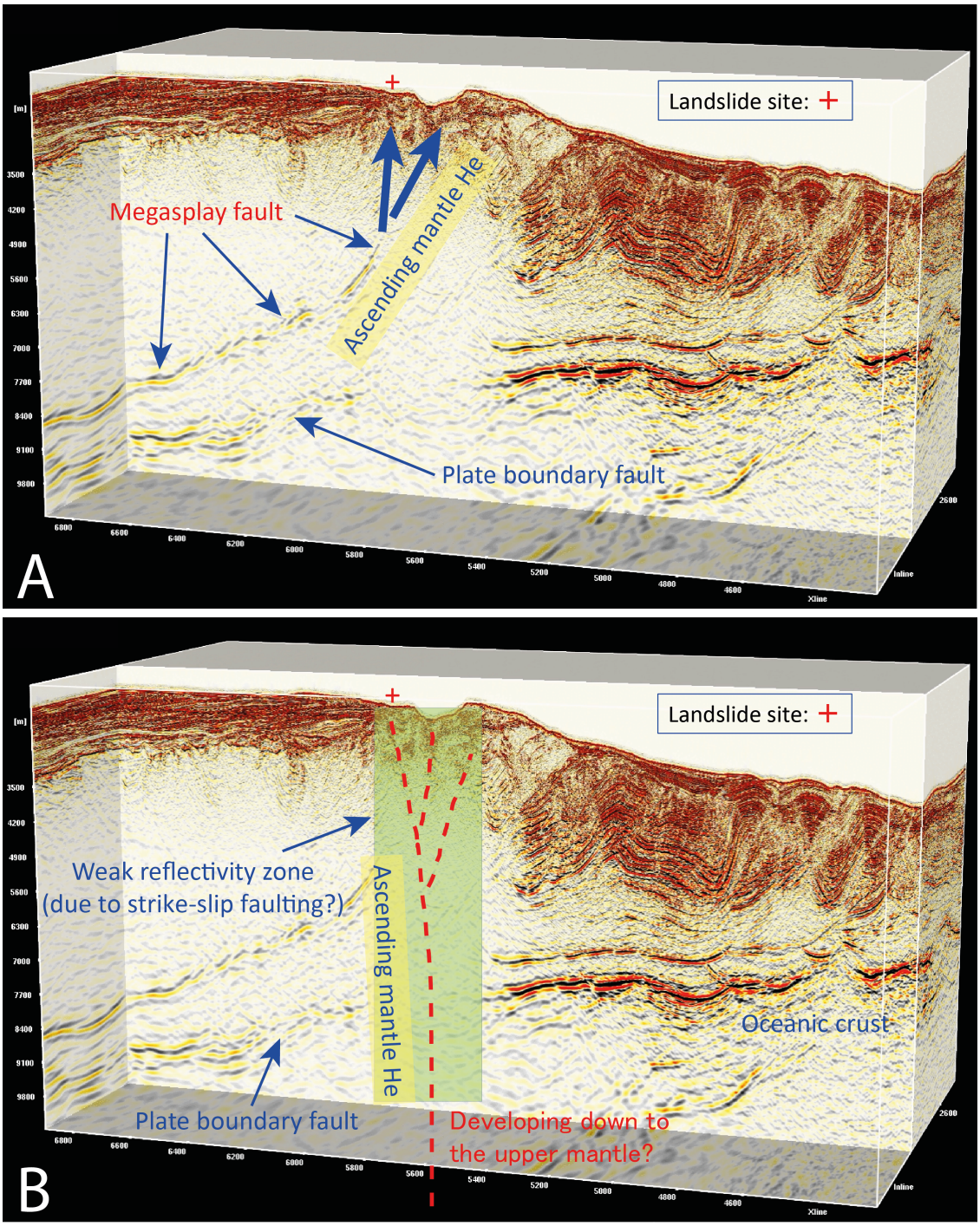

Figure 4: Illustration of the two scenarios proposed to explain the presence of mantle He in the Kumano Basin and in its surroundings based on 3D seismic profiles (see the work by Park et al.[37] for details) available for the Landslide site (i.e., IODP Site C0002). A) Extension of the megasplay fault along the plate boundary fault fostering the horizontal migration of fluids from the mantle wedge (note the steeper megasplay fault below the site Landslide). B) Strike-slip faults developing down into the subducting Philippine Sea Plate.

$^3He/^4He$ isotope ratios of 7–8 Ra to fluids derived from a deep mantle component beneath the Philippine Sea Plate. Based on this hypothesis, the observed high He isotope ratio could be also the result of a slab tear (i.e., favoring the second scenario mentioned above).

All measured water samples are slightly enriched in ^3He. However, because of the strong mixing generally occurring in the water column, both the concentrations and the isotope ratios are similar (see Figs. 2 and 3). Therefore, the respective data do not deliver site-specific insights. This underlines the potential of noble-gas analysis in the sediment pore water to characterize local/regional terrigenic fluid emission at the ocean floor.

Conclusions

Our study shows that the terrigenic fluid emission along the Nankai Trough is quite heterogeneous both in terms of He fluxes and origins. At sampling sites located between the outer ridge and the trench, mainly He of crustal origin was found in the acquired cores. In contrast, high He isotope ratios ranging from 2.4 Ra up to 4.4 Ra are found at shallower depths within the forearc region indicating the emission of mantle fluids.

Our findings suggest that deep-seated fluids from the mantle can be transported though preferential pathways up to the seafloor. Thus, within the context of studies targeting the relations between geochemistry and active tectonics, it could be meaningful to monitor geochemical changes in the noble-gas composition of the pore fluids even at shallow sediment depths.

Acknowledgement

Thanks are due to the NT13-08 and NT14-07 cruise members for their support during the sampling campaigns. We would like to thank Dr. Füri and an anonymous reviewer for their valuable comments on the manuscript. This research was supported by funding from the EU Seventh Framework Programme for Research and Technological Development (Marie Curie

International Outgoing Fellowship to YT, Contract PIOF-GA-2012-332404).

References

(1) Sano, Y.; Hara, T.; Takahata, N.; Kawagucci, S.; Honda, M.; Nishio, Y.; Tanikawa, W.; Hasegawa, A.; Hattori, K. Helium anomalies suggest a fluid pathway from mantle to trench during the 2011 Tohoku-Oki earthquake. *Nat. Commun.* **2014**, *5*.

(2) Sano, Y.; Takahata, N.; Kagoshima, T.; Shibata, T.; Onoue, T.; Zhao, D. Groundwater helium anomaly reflects strain change during the 2016 Kumamoto earthquake in Southwest Japan. *Sci. Rep.* **2016**, *6*, 37939.

(3) Hensen, C. et al. Marine Transform Faults and Fracture Zones: A Joint Perspective Integrating Seismicity, Fluid Flow and Life. *Front. Earth Sci.* **2019**, *7*, 39.

(4) Caracausi, A.; Paternoster, M. Radiogenic helium degassing and rock fracturing: A case study of the southern Apennines active tectonic region. *J. Geophys. Res.-Sol. Ea.* **2015**, *120*, 2200–2211.

(5) Buttitta, D.; Caracausi, A.; Chiaraluce, L.; Favara, R.; Morticelli, F. G.; Sulli, A. Continental degassing of helium in an active tectonic setting (northern Italy): the role of seismicity. *Sci. Rep.* **2020**, *10*, 162.

(6) Barnes, R. O.; Bieri, R. H. Helium Flux through Marine Sediments of the Northern Pacific Ocean. *Earth Planet. Sci. Lett.* **1976**, *28*, 331–336.

(7) Chaduteau, C.; Jean-Baptiste, P.; Fourré, E.; Charlou, J. L.; Donval, J. P. Helium transport in sediment pore fluids of the Congo-Angola margin. *Geochem. Geophy. Geosy.* **2009**, *10*.

(8) Lan, T. F.; Sano, Y.; Yang, T. F.; Takahata, N.; Shirai, K.; Pinti, D. L. Evaluating

Earth degassing in subduction zones by measuring helium fluxes from the ocean floor. *Earth Planet. Sci. Lett.* **2010**, *298*, 317–322.

(9) Sano, Y.; Wakita, H. Helium isotopes and heat flow on the ocean floor. *Chem. Geol.* **1987**, *66*, 217–226.

(10) Sayles, F. L.; Jenkins, W. J. Advection of Pore Fluids Through Sediments in the Equatorial East Pacific. *Science* **1982**, *217*, 245–248.

(11) Toki, T.; Maegawa, K.; Tsunogai, U.; Kawagucci, S.; Takahata, N.; Sano, Y.; Ashi, J.; Kinoshita, M.; Gamo, T. In *Accretionary Prisms and Convergent Margin Tectonics in the Northwest Pacific Basin*; Ogawa, Y., Anma, R., Dilek, Y., Eds.; Modern Approaches in Solid Earth Sciences; Springer: Netherlands, 2011; Vol. 8; pp 247–262.

(12) Tomonaga, Y.; Brennwald, M. S.; Kipfer, R. Using helium and other noble gases in ocean sediments to characterize active methane seepage off the coast of New Zealand. *Mar. Geol.* **2013**, *344*, 34–40.

(13) Seno, T.; Stein, S.; Gripp, A. E. A model for the motion of the Philippine Sea Plate consistent with NUVEL-I and geological data. *J. Geophys. Res.* **1993**, *98*, 941–948.

(14) Loveless, J. P.; Meade, B. J. Geodetic imaging of plate motions, slip rates, and partioning of deformation in Japan. *J. Geophys. Res.* **2010**, *115*, B02410.

(15) Davis, E.; Becker, K.; Wang, K.; Obara, K.; Ito, Y.; Kinoshita, M. A discrete episode of seismic and aseismic deformation of the Nankai trough subduction zone accretionary prism and incoming Philippine Sea plate. *Earth Planet. Sci. Lett.* **2006**, *242*, 73–84.

(16) Burnard, P.; Zimmermann, L.; Sano, Y. *The Noble Gases as Geochemical Tracers*; Advances in Isotope Geochemistry; Springer: Berlin, Heidelberg, 2013; pp 1–15.

(17) Wiersberg, T.; Hammerschmidt, S. B.; Fuchida, S.; Kopf, A.; Erzinger, J. Mantle-derived fluids in the Nankai Trough Kumano forearc basin. *Progress in Earth and Planetary Science* **2018**, *5*.

(18) Toki, T.; Tsunogai, U.; Gamo, T.; Kuramoto, S.; Ashi, J. Detection of low-chloride fluids beneath a cold seep field on the Nankai accretionary wedge off Kumano, south of Japan. *Earth Planet. Sci. Lett.* **2004**, *228*, 37–47.

(19) Kuramoto, S. In *R/V Natsushima NT02-08 Cruise Report*; Kuramoto, S., Ed.; Japan Marine Science and Technology Center, 2002; pp 63–73.

(20) Yagasaki, K.; Ashi, J.; Yokoyama, Y.; Obrochta, S.; Miyairi, Y.; Kuramoto, S. Evidence for Tokai fault segment ruptures of the Nankai Trough from a colossal methanogenic sub-fossil bivalve grave. **2020**, in preparation.

(21) Wen, H.; Sano, Y.; Takahata, N.; Tomonaga, Y.; Ishida, A.; Tanaka, K.; Kagoshima, T.; Shirai, K.; Ishibashi, J.; Yokose, H.; Tsunogai, U.; Yang, T. F. Helium and methane sources and fluxes of shallow submarine hydrothermal plumes near the Tokara Islands, Southern Japan. *Sci. Rep.* **2016**, *6*, 34126.

(22) Brennwald, M. S.; Hofer, M.; Peeters, F.; Aeschbach-Hertig, W.; Strassmann, K.; Kipfer, R. Analysis of dissolved noble gases in the pore water of lacustrine sediments. *Limnol. Oceanogr.: Methods* **2003**, *1*, 51–62.

(23) Beyerle, U.; Aeschbach-Hertig, W.; Imboden, D. M.; Baur, H.; Graf, T.; Kipfer, R. A mass spectrometric system for the analysis of noble gases and tritium from water samples. *Environ. Sci. Technol.* **2000**, *34*, 2042–2050.

(24) Tomonaga, Y.; Brennwald, M. S.; Kipfer, R. An improved method for the analysis of dissolved noble gases in the pore water of unconsolidated sediments. *Limnol. Oceanogr.: Methods* **2011**, *9*, 42–49.

(25) Brennwald, M. S.; Vogel, N.; Scheidegger, Y.; Tomonaga, Y.; Livingstone, D. M.; Kipfer, R. In *The Noble Gases as Geochemical Tracers*; Burnard, P., Hoefs, J., Eds.; Advances in Isotope Geochemistry; Springer: Berlin, Heidelberg, 2013; pp 123–153.

(26) Tomonaga, Y.; Brennwald, M. S.; Meydan, A. F.; Kipfer, R. Noble gases in the sediments of Lake Van – solute transport and palaeoenvironmental reconstruction. *Quat. Sci. Rev.* **2014**, *104*, 117–126.

(27) Sano, Y.; Wakita, H. Precise measurement of helium isotopes in terrestrial gases. *B. Chem. Soc. Jpn.* **1988**, *61*, 1153–1157.

(28) Matsuda, J.; Matsumoto, T.; Sumino, H.; Nagao, K.; Yamamoto, J.; Miura, Y.; Kaneoka, I.; Takahata, N.; Sano, Y. The $^{3}He/^{4}He$ ratio of the new internal He Standard of Japan (HESJ). *Geochem. J.* **2002**, *36*, 191–195.

(29) Park, J.-O.; Tsuru, T.; Kodaira, S.; Cummins, P. R.; Kaneda, Y. Splay fault branching along the Nankai subduction zone. *Science* **2002**, *297*, 1157–1160.

(30) Ozima, M.; Podosek, F. A. *Noble gas geochemistry*; Cambridge University Press: Cambridge, London, New York, 1983.

(31) Dogan, T.; Sumino, H.; Nagao, K.; Notsu, K. Release of mantle helium from the forearc region of the Philippine Sea plate subduction. *Chem. Geol.* **2006**, *233*, 235–248.

(32) Sano, Y.; Fischer, T. P. In *The Noble Gases as Geochemical Tracers*; Burnard, P., Hoefs, J., Eds.; Advances in Isotope Geochemistry; Springer: Berlin, Heidelberg, 2013; pp 249–317.

(33) Torgersen, T.; Lupton, J. E.; Sheppard, D. S.; Giggenbach, W. F. Helium isotope variations in the thermal areas of New Zealand. *J. Volcanol. Geotherm. Res.* **1982**, *12*, 283–298.

(34) Kipfer, R.; Aeschbach-Hertig, W.; Peeters, F.; Stute, M. In *Noble Gases in Geochemistry and Cosmochemistry*; Porcelli, D., Ballentine, C., Wieler, R., Eds.; Reviews in Mineralogy and Geochemistry; Mineralogical Society of America, Geochemical Society, 2002; Vol. 47; pp 615–700.

(35) Talley, L. D. In *Hydrographic Atlas of the World Ocean Circulation Experiment (WOCE). Volume 2: Pacific Ocean*; Sparrow, M., Chapman, P., Gould, J., Eds.; International WOCE Project Office: Southampton, U.K., 2007.

(36) Takahata, N.; Tomonaga, Y.; Kumamoto, Y.; Yamada, M.; Sano, Y. Direct tritium emissions to the ocean from the Fukushima Dai-ichi nuclear accident. *Geochem. J.* **2018**, *52*, 211–217.

(37) Park, J.-O.; Fujie, G.; Wijerathne, L.; Hori, T.; Kodaira, S.; Fukao, Y.; Moore, G. F.; Bangs, N. L.; Kuramoto, S.; Taira, A. A low-velocity zone with weak reflectivity along the Nankai subduction zone. *Geology* **2010**, *38*, 283–286.

(38) Ashi, J.; Lallement, S.; Masago, H. NanTroSEIZE megasplay riser pilot. *IODP Scientific Prospectus* **2007**, *315*.

(39) Kennedy, B. M.; Kharaka, Y. K.; Evans, W. C.; Ellwood, A.; DePaolo, D. J.; Thordsen, J.; Ambats, G.; Mariner, R. H. Mantle fluids in the San Andreas fault system, California. *Science* **1997**, *278*, 1278–1281.

(40) Füri, E.; Hilton, D. R.; Brown, K. M.; Tryon, M. D. Helium systematics of cold seep fluids at Monterey Bay, California, USA: Temporal variations and mantle contributions. *Geochem. Geophy. Geosy.* **2009**, *10*, Q08013.

(41) Lee, H.; Kim, H.; Kagoshima, T.; Park, J.-O.; Takahata, N.; Sano, Y. Mantle degassing along strike-slip faults in the Southeastern Korean Peninsula. *Sci. Rep.* **2019**, *9*, 15334.

(42) Barry, P. H. et al. Forearc carbon sink reduces long-term volatile recycling into the mantle. *Nature* **2019**, *568*, 487–492.

(43) Sano, Y.; Kameda, A.; Takahata, N.; Yamamoto, J.; Nakajima, J. Tracing extinct spreading center in SW Japan by helium-3 emanation. *Chem. Geol.* **2009**, *266*, 50–56.

For TOC Only